Available online at www.sciencedirect.com
ScienceDirect
Journal of the European Ceramic Society 30 (2010) 1253–1258
www.elsevier.com/locate/jeurceramsoc

Structural characterization of TiO_2–P_2O_5–CaO glasses by spectroscopy

A.M.B. Silva [a,b], R.N. Correia [a,b], J.M.M. Oliveira [c,b], M.H.V. Fernandes [a,b,*]

[a] Department of Ceramics and Glass Engineering, University of Aveiro, 3810-193 Aveiro, Portugal
[b] Centre for Research in Ceramics and Composite Materials, CICECO, University of Aveiro, 3810-193 Aveiro, Portugal
[c] High School of North-Aveiro, University of Aveiro, Edifício Rainha, 5° Andar, 3720-232 Oliveira de Azeméis, Portugal

Received 14 May 2009; received in revised form 14 October 2009; accepted 2 November 2009
Available online 2 December 2009

Abstract

The structure of glasses with composition x TiO_2·(65 − x) P_2O_5·35 CaO (x = 0–30 mol%) has been studied and their glass transition temperature, Raman and NMR spectra have been analysed.

For TiO_2-free glass two phosphate species have been identified as Q^2 and Q^3. Increasing TiO_2 content in glass compositions results in the disappearance of the Q^3 and Q^2 species and in the formation of, mainly, pyrophosphate structure, Q^1.

In calcium titanophosphate glass with higher TiO_2 content the structure consists of a distorted Ti octahedral linked to pyrophosphate unit through P–O–Ti bonds. In these glass series the structural cohesion increases with TiO_2, although a depolymerization in the original P–O–P network occurs.

The study of these glasses and the understanding of their structural characteristics can give a valuable contribution for the clarification of their degradation behaviour namely in biological environments.

Keywords: Glass; TiO_2; Spectroscopy; Structure; Biomedical applications

1. Introduction

Phosphate glasses can be analyzed as a polymer-like, regular tetrahedral network based on [PO_4] groups, with their structure generally described using Q^n terminology, where n represents the number of bridging oxygens per tetrahedron.[1–3]

Depending on the [O]/[P] ratio as set by glass composition, the phosphate glasses can be described by different structures: cross-linked network of Q^3 tetrahedra (vitreous P_2O_5); polymer-like metaphosphate chains of Q^2 tetrahedra; 'invert' glasses based on small pyro (Q^1) and orthophosphate (Q^0) species.[1,4,5]

The addition of a modifier oxide leads to the creation of non-bridging oxygens in the glass resulting in the depolymerization of the phosphate network, with oxygen atoms breaking the P–O–P links. This breakage in the structure of phosphate glass generally decreases and weakens some of their properties, namely, mechanical and chemical properties.[1,6,7]

Almost all bioactive glass-based materials contain a large amount of silica, but the development of new glass-ceramic biomaterials has recently concentrated on SiO_2-free glasses. It is well accepted that phosphate-based glasses without silica and with high CaO/P_2O_5 molar ratio (>1.5) exhibit a high potential for use as biomaterials.[4,8–10]

Some authors argue that this capability comes from the fact that these calcium phosphate glasses have chemical compositions close to that of hard tissues.[11,12] Chemical stability of these glasses is not properly known. Although many researchers reported the dissolution behavior in living body of calcium phosphate glasses near the metaphosphate composition,[13–15] there are no studies on their bioactivity. The solubility behavior of these phosphate glasses can be controlled by modifying their chemical composition[9] or by promoting adequate heat treatments that produce the precipitation of crystals in the glasses with the required phases and sizes and allow the control of microstructure.[16,17]

Special cautions are needed in the preparation of these glasses because they often exhibit hygroscopicity and high tendency to crystallize. Preparation of calcium phosphate glasses in the

* Corresponding author at: Department of Ceramics and Glass Engineering, University of Aveiro, 3810-193 Aveiro, Portugal. Tel.: +351 234370240; fax: +351 234425300.
E-mail addresses: ambsilva@ua.pt (A.M.B. Silva), rcorreia@ua.pt (R.N. Correia), martinho@ua.pt (J.M.M. Oliveira), helena.fernandes@ua.pt (M.H.V. Fernandes).

0955-2219/$ – see front matter © 2009 Elsevier Ltd. All rights reserved.
doi:10.1016/j.jeurceramsoc.2009.11.001

pyro or orthophosphate region ($CaO/P_2O_5 \approx 2$ or 3) has been achieved only by using large amounts of other oxides such as TiO_2,[10,18–21] TiO_2 and Na_2O,[11,16,22] B_2O_3,[8] or TiO_2, MgO and Na_2O.[23–26]

Titanium oxide does not form a glass alone, but it can be incorporated in significant amounts into other glass-forming oxide systems such as phosphates.[27–29] The addition of TiO_2 to phosphate glasses contributes to improve glass-forming ability, chemical durability and stabilization of the glass structure.[12,22,28–30]

In these glasses, titanium ions can also participate in the network formation, although they have a coordination number higher than 4.[22] In the early investigations of TiO_2–P_2O_5,[27] $NaPO_3$–TiO_2[31] and Na_2O–TiO_2–P_2O_5[32] glasses, it was found that titanium is present in the octahedral coordination (TiO_6).

Previous reports on the preparation of glass and glass-ceramics in the CaO–P_2O_5–TiO_2 system have indicated that biocompatible and bioactive phases may be produced.[33,34] In this system, a new family of phosphate glass-ceramics appears with a mixture of soluble and less soluble crystalline phases such as β-$Ca_2P_2O_7$ and $CaTiO_4(PO_4)_6$, respectively.[26,35–37]

The aim of the present study is to understand the structure of glasses belonging to the TiO_2–P_2O_5–CaO system. Raman and Magic Angle Spinning Nuclear Magnetic Resonance (MAS-NMR) spectroscopy were used to study the structural evolution of the glasses as a function of composition.

This study will be further used to understand the behavior of these glasses in fluids, aiming to use them in biomedical applications.

2. Materials and methods

Glasses with molar compositions $x TiO_2 \cdot (65 - x)\ P_2O_5 \cdot 35$ CaO, with $0 < x < 30$ mol%, were prepared from reagent grade TiO_2, P_2O_5 and $Ca(H_2PO_4)_2 \cdot H_2O$. Batches were placed in a plastic flask and stirred for 45 min to allow homogeneization.

The mixtures were put in a platinum crucible, melted at temperatures between 1000 and 1500 °C in an electrical furnace from 1 to 1.5 h, in agreement with TiO_2 content increase. As the P_2O_5-volatility may be a concern, particularly when crystalline P_2O_5 is used as a raw material, Scanning Electron Microscope/Energy Dispersive System (SEM/EDS) analysis were performed in some of the obtained samples to assess glass compositions. For all tested glass samples compositions were within an experimental error of 3 mol% maximum. Each melt batch was poured into water in order to quench and produce a glass frit. The frit was dried at 60 °C during 48 h and then reduced to powder.

Powder X-ray diffractometry (XRD) was used to confirm the amorphous state of the samples.

Differential thermal analysis (DTA) was carried out at 5 and 10 °C/min, to assess the glass transition temperature, Tg.

Glass powders were used for Raman spectroscopy measurements. Spectra were recorded at room temperature in the range of 0–1500 cm^{-1} using a FT-Raman Bruker spectrometer. All measurements were run at 4 cm^{-1} resolution.

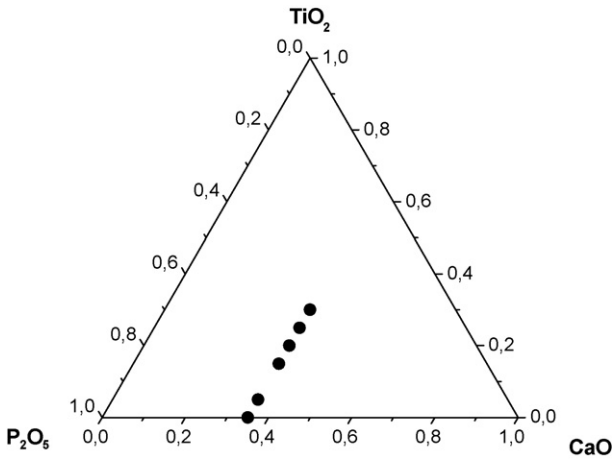

Fig. 1. Investigated glasses in the TiO_2–P_2O_5–CaO system.

^{31}P MAS-NMR spectra of the powder glasses were recorded using a NMR spectrometer Bruker, Avance 400, operating at 161.97 MHz with 45° pulses, spinning rates of 10 kHz, a 45 s recycle delay and the chemical shift was quoted in ppm from phosphoric acid (85%).

3. Results

Fig. 1 shows the investigated glass compositions ($x TiO_2 \cdot (65 - x)\ P_2O_5 \cdot 35$ CaO, with $x = 0$–30 mol%), on the ternary diagram TiO_2–P_2O_5–CaO. The CaO content is fixed at 35 mol% and P_2O_5 is gradually replaced by TiO_2 in a molar base.

The studied compositions and O/P ratio are listed in Table 1. The amorphous state of all samples was confirmed by XRD analyses.

TiO_2-free composition gives a transparent glass, but the addition of TiO_2 by replacing P_2O_5 produces a gradual coloration of the samples, from a clear pink for the small portion of TiO_2.

Fig. 2 shows the effect of TiO_2 content on the transition temperature, Tg being evident that the increase of TiO_2 content increases the Tg values. The observed results give a first indication that glasses with higher TiO_2 percentage are likely to exhibit a higher structural cohesion.

Fig. 3(a) and (b) shows, respectively, Raman and ^{31}P MAS-NMR spectra of $x TiO_2 \cdot (65 - x)\ P_2O_5 \cdot 35$ CaO glasses ($x = 0$–30 mol%).

Table 1
Composition and O/P ratio of investigated TiO_2–P_2O_5–CaO glasses.

Sample identification	TiO_2 (mol%)	P_2O_5 (mol%)	CaO (mol%)	Ratio O/P
T00P65	0	65	35	2.77
T05P60	5	60	35	2.88
T15P50	15	50	35	3.15
T20P45	20	45	35	3.33
T25P40	25	40	35	3.56
T30P35	30	35	35	3.86

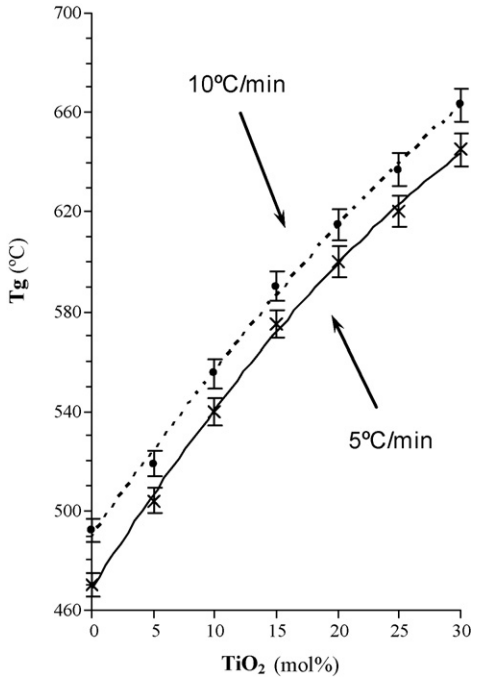

Fig. 2. Glass transition temperature of $x\mathrm{TiO_2}\cdot(65-x)\ \mathrm{P_2O_5}\cdot 35$ CaO glasses obtained by DTA at 5 °C/min and 10 °C/min.

Raman spectrum of T00P65 glass, Fig. 3(a), exhibit strong bands at ∼680, ∼1175 and ∼1290 $\mathrm{cm^{-1}}$ and a broad band in the spectral region 280–380 $\mathrm{cm^{-1}}$. TiO_2 introduction in glass composition changes Raman spectra, a situation that becomes more evident for higher TiO_2 contents. All these bands have a tendency to disappear and new ones at 765 and 920 $\mathrm{cm^{-1}}$ are observed for higher TiO_2 contents. A resume of the Raman bands and the proposed assignments is shown in Table 2.

^{31}P MAS-NMR spectra, Fig. 3(b), shows that the increase of TiO_2 content in the glass composition produces the shift of the peak towards higher frequencies. The obtained ^{31}P MAS-NMR spectra were decomposed into Gaussian contributions of different isotropic peaks and the results for the several glass compositions are listed in Table 3, Isotropic peaks are labeled with Q^n values where n represents the number of bridging oxygen per phosphate tetrahedron. An example of this decomposition is represented in Fig. 4 for T30P35 glass.

Table 2
Positions ($\mathrm{cm^{-1}}$) of Raman bands and proposed assignments for $x\mathrm{TiO_2}\cdot(65-x)\ \mathrm{P_2O_5}\cdot 35$ CaO glasses ($x = 0$–30 mol%).[2,7,11,22,23,32,38–46].

Position ($\mathrm{cm^{-1}}$)	Assignment
∼320	Bend mode of phosphate polyhedron
∼522	(POP) bending
∼630	$(POP)_{sym}$ stretch (bridging oxygen), or TiO_6 unit
∼680	$(POP)_{sym}$ stretch (bridging oxygen), Q^2 species
∼765	$(POP)_{sym}$ stretch (bridging oxygen), Q^1 species, or distorted TiO_6 octahedron
∼920	Ti–O stretch (non-bridging oxygen) (TiO_5 unit)
∼995	$(PO_4)_{sym}$ stretch (non-bridging oxygen), Q^0 species
∼1040	$(PO_3)_{sym}$ stretch (non-bridging oxygen), Q^1 species
∼1175	$(PO_2)_{sym}$ stretch (non-bridging oxygen), Q^2 species
∼1290	$(PO_2)_{asym}$ stretch (non-bridging oxygen), Q^2 species
∼1325	$(P{=}O)_{sym}$ stretch

4. Discussion

In Raman spectrum of T00P65 glass the band at 680 $\mathrm{cm^{-1}}$ is assigned to the symmetric stretching motion of bridging oxygen, ν_s (POP), in Q^2 phosphate tetrahedron. The 1175 and 1290 $\mathrm{cm^{-1}}$ bands correspond to the symmetric, ν_s, and asymmetric, ν_{as}, stretching motions, respectively, of two non-bridging oxygen bonded to phosphorus (PO_2), in Q^2 phosphate tetrahedron. The broad band at ∼320 $\mathrm{cm^{-1}}$ has been assigned to bending vibrations, δ, of phosphate polyhedra. Raman spectrum of this glass (T00P65) matches a typical Raman pattern of a metaphosphate glass composition.[2,23,38–43]

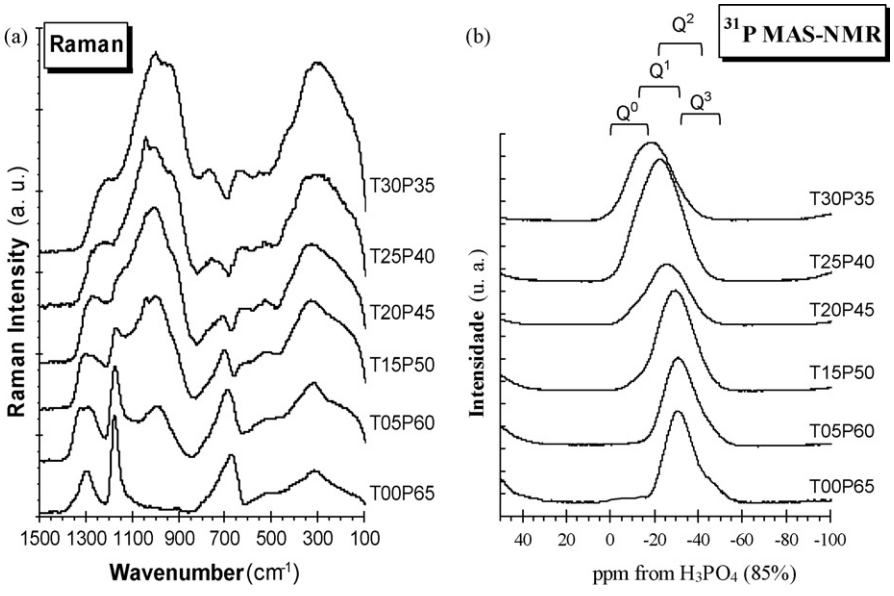

Fig. 3. (a) Raman and (b) ^{31}P MAS-NMR spectra of $x\mathrm{TiO_2}\cdot(65-x)\ \mathrm{P_2O_5}\cdot 35$ CaO glasses.

Table 3
^{31}P MAS-NMR spectra decomposed for the several glass compositions and Q^0, Q^1, Q^2 and Q^3 peaks with respective fractional areas (chemical shift: ppm from H_3PO_4 (85%)).

Glass	Q^3 chemical shift (ppm) (fractional area)	Q^2 chemical shift (ppm) (fractional area)	Q^1 chemical shift (ppm) (fractional area)	Q^0 chemical shift (ppm) (fractional area)
T00P65	∼−44 (∼19%)	∼−31 (∼81%)	–	–
T05P60	∼−43 (∼16%)	∼−30 (∼84%)	–	–
T15P50	–	∼−33 (∼15%)	∼−28 (∼82%)	∼−10 (∼3%)
T20P45	–	–	∼−26 (∼97%)	∼−10 (∼3%)
T25P40	–	–	∼−23 (∼97%)	∼−11 (∼3%)
T30P35	–	–	∼−20 (∼88%)	∼−11 (∼12%)

It is observed that relative intensities of 680, 1175 and 1290 cm^{-1} bands decrease as TiO_2 content increases. When 5 mol% TiO_2 is added to that glass composition, Raman spectrum exhibit the same bands of T00P65 glass and two new bands, one at ∼995 and another at ∼1325 cm^{-1}. The band at 995 cm^{-1} is assigned to the symmetric stretching mode of non-bridging oxygen (PO_4^-) in Q^0 tetrahedron[23,42–44] and the band at 1325 cm^{-1} is assigned to stretching P=O bonds.[2,39]

Addition of 15 mol% TiO_2 to the base glass composition results in a small shift of the 680 band to 700 cm^{-1}, with lower relative intensity, and the appearance of new bands at ∼1040, ∼522 and a weak band at 630 cm^{-1}. The shift in the frequency of the band is attributed to a change in the in-chain P–O–P bond angle depending on the effect of the network modifier on phosphate glass structure.[38] In principle these new bands in T15P50 glass spectrum could be related with the incorporation of titanium atoms in the phosphate glass network. The 1040 cm^{-1} band is due to the motion of the non-bridging oxygen (PO_3) in Q^1 tetrahedron[1,8,42,45] and the 522 cm^{-1} band is attributed to the bending vibration (δ) of P-O bonds.[2,22,23] Some authors refer that 630 cm^{-1} band is associated to regions where vibrations of P–O–P bridges are expected, but it is also reported that this band can be related to another group composed of titanium–oxygen units, the TiO_6 group.[7,11,40,46]

Glasses with higher TiO_2 content exhibit the same bands in the Raman spectra. Increase of TiO_2 content results in a small shift of the 1280 band to 1200 cm^{-1} and a tendency for the disappearance of the 700 and 1175 cm^{-1} bands. The intensity of the 630 cm^{-1} band increases with TiO_2 and becomes more distinct in the T30P35 glass spectrum. New bands at 765 and 920 cm^{-1} appear for T25P40 and T30P35 glasses. Some authors defend that 765 cm^{-1} band refers to the motion of bridging oxygen (POP) in Q^1 tetrahedron[42] but it is also reported that this band can be ascribed to distorted TiO_6 octahedron, as proposed by Krimi.[23,32] The band at 920 cm^{-1} could be attributed either to non-bridging oxygen in Ti–O stretching vibration in TiO_4 units containing non-bridging oxygen[11,46] or to a short Ti–O bond on a distorted TiO_5 site.[32] This point will become clear after the analysis of the ^{31}P MAS-NMR spectra.

^{31}P MAS-NMR spectra, Fig. 3(b) and Table 3, shows that the peak shifts towards higher frequencies as TiO_2 increases. This suggests that depolymerization of the phosphate network becomes higher as the TiO_2 content increases.

In the TiO_2-free glass (T00P65) the presence of two species of phosphate tetrahedra (Q^2 and Q^3) is highly probable. This glass is dominated by an isotropic peak near −31 ppm, representing Q^2 tetrahedral (metaphosphate chains), Fig. 5 and Table 3. In the decomposed spectrum of this glass another peak is found, with lower intensity centered at −44 ppm associated to Q^3 species.[1,47]

The introduction of TiO_2 in calcium phosphate glasses changes the ^{31}P MAS-NMR spectrum. This is explained by the break of P=O bonds and the formation of P–O–Ti bonds, as represented in Fig. 6. For the composition with 15 mol% TiO_2 (T15P50) a structure consisting of Ti octahedral linked to metaphosphate and pyrophosphate units is proposed. Gaussian decomposition of spectrum seems to indicate the presence of a small amount of orthophosphate units, Table 3. Those structures are based on $P_2O_6^{2-}$ and $P_2O_7^{4-}$ groups, as represented in Figs. 5 and 7.[30]

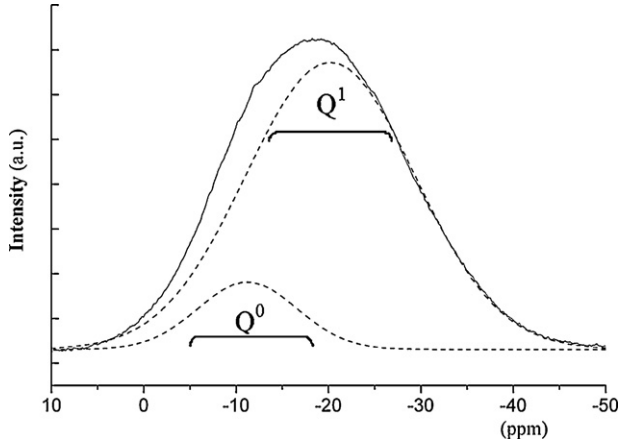

Fig. 4. Decomposed ^{31}P MAS-NMR spectrum for T30P35 glass.

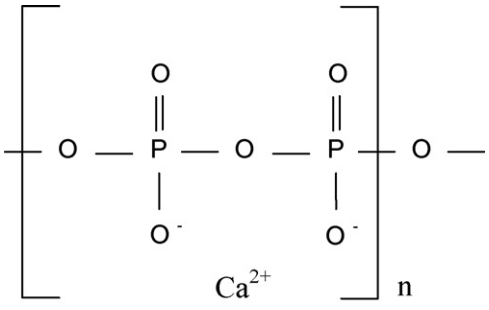

Fig. 5. Metaphosphate chain glass structure.

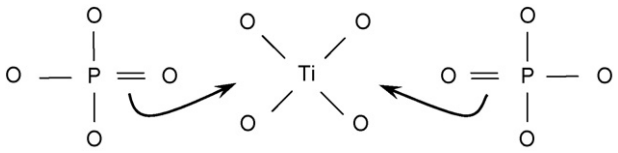

Fig. 6. Break of P=O bonds and formation of P–O–Ti bonds.

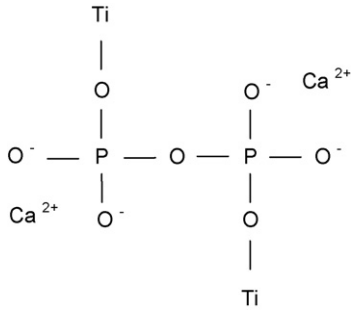

Fig. 7. Ti linked to the pyrophosphate units.

For the two glass compositions with higher TiO_2 content (T25P40 and T30P35) and since $O/P \geq 3.5$ no Q^2 sites will remain in the phosphate network and the formation of Q^1 and Q^0 sites is more likely.[30] So, there is no evidence of the presence of TiO_4 units. It is rather accepted that Ti is present in the form of TiO_6 and TiO_5 units. In these circumstance, the band at 920 cm^{-1} found in the Raman spectra should be assigned to a short Ti–O bond on a distorted TiO_5 site.

The previous analysis shows that in the glass series of the present study the addition of TiO_2 to a calcium phosphate glass produces the evolution of the glass network from a mixed cross-linked Q^3 species and a chain-like Q^2 species to a network dominated by Q^1 units. However, contrarily to what would be expected due to depolymerization, it is observed that the addition of TiO_2 produces the enhancement of the glass structure cohesion as suggested by the Tg trend. This behaviour was attributed to structural rearrangements in the main phosphate network due to the replacing of P–O–P by Ti–O–P bonds.

5. Conclusions

Raman and ^{31}P MAS-NMR spectroscopic methods have revealed the features of the internal structure of glasses with compositions $x TiO_2 \cdot (65 - x)\ P_2O_5 \cdot 35\ CaO$ ($x = 0$–30 mol%).

Chain phosphate units dominate the structure of TiO_2-free and TiO_2 lower contents, near the metaphosphate composition.

Pyrophosphate units dominate the glass structure for higher TiO_2 contents.

All calcium phosphate glasses containing TiO_2 exhibit P–O–Ti bonds that increase with TiO_2 content.

A progressive depolymerization of the phosphate glass network occurs as TiO_2 content increases but the cohesion of glass structure increases due to the replacing of P–O–P bonds by Ti–O–P bonds.

Acknowledgements

The authors acknowledge the Portuguese Foundation of Science and Technology for the financial support through the project POCI/CTM/60761/2004.

References

1. Brow RK. Review: the structure of simple phosphate glasses. *J Non-Cryst Solids* 2000;**263 & 264**:1–28.
2. Meyer K. Characterization of the structure of binary zinc ultraphosphate glasses by infrared and Raman spectroscopy. *J Non-Cryst Solids* 1997;**209**(3):227–39.
3. Hartmann P, Vogel J, Schnabel B. NMR study of phosphate glasses and glass ceramic structures. *J Non-Cryst Solids* 1994;**176**(2–3):157–63.
4. Dias AG, Lopes MA, Gibson IR, Santos JD. In vitro degradation studies of calcium phosphate glass ceramics controlled crystallization. *J Non-Cryst Solids* 2003;**330**(1–3):81–9.
5. Walter G, Vogel J, Hoppe U, Hartmann P. The structure of $CaO–Na_2O–MgO–P_2O_5$ invert glass. *J Non-Cryst Solids* 2001;**296**(3):212–23.
6. Clément J, Manero JM, Planell JA, Avila G, Martínez S. Analysis of the structural changes of a phosphate glass during its dissolution in simulated body fluid. *J Mater Sci: Mater Med* 1999;**10**:729–32.
7. Hoppe U, Brow RK, Tischendorf BC, Kriltz A, Jóvári P, Schöps A, Hannon AC. Structure of titanophosphate glasses studied by X-ray and neutron diffraction. *J Non-Cryst Solids* 2007;**353**(18–21):1802–7.
8. Saranti A, Koutselas I, Karakassides MA. Bioactive glasses in the system $CaO–B_2O_3–P_2O_5$: preparation, structural study and in vitro evaluation. *J Non-Cryst Solids* 2006;**352**(5):390–8.
9. Franks K, Abrahams I, Knowles JC. Development of soluble glasses for biomedical use. Part I. In vitro solubility measurement. *J Mater Sci: Mater Med* 2000;**11**:609–14.
10. Zhang Y, Lopes MA, Santos JD. $CaO–P_2O_5$ glass ceramics containing bioactive phases: crystallisation and in vitro bioactivity studies. *Bioceram Key Eng Mater* 2001;**192–195**:643–8.
11. Kasuga T, Abe Y. Calcium phosphate invert glasses with soda and titania. *J Non-Cryst Solids* 1999;**243**(1):70–4.
12. Kasuga T. Bioactive calcium pyrophosphate glasses and glass-ceramics. *Acta Biomater* 2005;**1**(1):55–64.
13. Uo M, Mizuno M, Kuboki Y, Makishima A, Watari F. Properties and cytotoxicity of water soluble $Na_2O–CaO–P_2O_5$ glasses. *Biomaterials* 1998;**19**(24):2277–84.
14. Pilliar RM, Filiaggi MJ, Wells JD, Grynpas MD, Kandel RA. Porous calcium polyphosphate scaffolds for bone substitute applications—in vitro characterization. *Biomaterials* 2001;**22**(9):963–72.
15. Brauer DS, Rüssel C, Kraft J. Solubility of glasses in the system $P_2O_5–CaO–MgO–Na_2O–TiO_2$: experimental and modeling using artificial neural networks. *J Non-Cryst Solids* 2007;**353**(3):263–70.
16. Kasuga T, Abe Y. Novel calcium phosphate ceramics prepared by powder sintering and crystallization of glasses in the pyrophosphate region. *J Mater Res* 1998;**13**(12):3357–60.
17. Franks K, Abrahams I, Georgiou G, Knowles JC. Investigation of thermal parameters and crystallisation in a ternary $CaO–Na_2O–P_2O_5$-based glass system. *Biomaterials* 2001;**22**(5):497–501.
18. Abe Y.*Proceedings of International Forum on Fine Ceramics'90*. 1990. p. 78.
19. Ohtsuki C, Osaka A, Kokubo T. Effect of Al_2O_3 and TiO_2 on bioactivity of $CaO–SiO_2$ glasses. *Bioceramics* 1994;**7**:73–8.
20. Rizkalla AS, Jones DW, Clarke DB, Hall GC. Crystallization of experimental bioactive glass compositions. *J Biomed Mater Res* 1996;**32**:119–24.
21. Navarro M, Clément J, Ginebra MP, Martínez S, Avila G, Planell JA. Improvement of the stability and mechanical properties of resorbable phosphate glasses by the addition of TiO_2. *Key Eng Mater* 2002;**218–220**:275–8.
22. Shaim A, Et-tabirou M. Role of titanium in sodium titanophosphate glasses and a model of structural units. *Mater Chem Phys* 2003;**80**(1):63–7.

23. Karakassides MA, Saranti A, Koutselas I. Preparation and structural study of binary phosphate glasses with high calcium and/or magnesium content. *J Non-Cryst Solids* 2004;**347**(1–3):69–79.
24. Zhang Y, Santos JD. Crystallization and microstructure analysis of calcium phosphate-based glass ceramics for biomedical applications. *J Non-Cryst Solids* 2000;**272**(1):14–21.
25. Zhang Y, Santos JD. Microstructural characterization and in vitro apatite formation in $CaO–P_2O_5–TiO_2–MgO–Na_2O$ glass-ceramics. *J Eur Ceram Soc* 2001;**21**(2):169–75.
26. Dias AG, Skakle JMS, Gibson IR, Lopes MA, Santos JD. In situ thermal and structural characterization of bioactive calcium phosphate glass ceramics containing TiO_2 and MgO oxides: high temperature—XRD studies. *J Non-Cryst Solids* 2005;**351**(10–11):810–7.
27. Brow RK, Tallant DR, Warren WL, McIntyre A, Day DE. Spectroscopic studies of the structure of titanophosphate and calcium titanophosphate glasses. *Phys Chem Glasses* 1997;**38**(6):300–6.
28. Kishioka A, Haba M, Amagasa M. Glass formation in multicomponent phosphate systems containing TiO_2. *Bull Chem Soc Jpn* 1974;**47**(10):2493–6.
29. Kishioka A. Glass formation in the $Li_2O–TiO_2–P_2O_5$, $MgO–TiO_2–P_2O_5$ and $CaO–TiO_2–P_2O_5$ systems. *Bull Chem Soc Jpn* 1978;**51**(9):2559–61.
30. Montagne L, Palavit G, Shaim A, Et-Tabirou M, Hartmann P, Jäger C. Structure and ionic conductivity of sodium titanophosphate glasses. *J Non-Cryst Solids* 2001;**293–295**:719–25.
31. Kishioka A, Rousselot C, Malugani JP, Mercier R. Ionic conductivity and structure in $NaPO_3–TiO_2$ glasses. *Phosphorus Res Bull* 1991;**1**:387–92.
32. Krimi S, El Jazouli A, Rabardel L, Couzi M, Mansouri I, Le Flem G. Glass formation in the $Na_2O–TiO_2–P_2O_5$ system. *J Solid-State Chem* 1993;**102**(2):400–7.
33. Abe Y, Hosono H, Hosoe M. Development of calcium phosphate glass-ceramics for surgical and dental use. *Phosphorus Sulfur Silicon Relat Elem* 1987;**30**(1–2):337–40.
34. Suzuki T, Toriyama M, Hosono H, Abe Y. Application of a microporous glass-ceramics with a skeleton of $CaTi_4(PO_4)_6$ to carriers for immobilization of enzymes. *J Ferment Bioeng* 1991;**72**:384–91.
35. Lin F-H, Lin C-C, Lu C-M, Liu H-C, Sun J-S, Wang C-Y. Mechanical properties and histological evaluation of sintered β-$Ca_2P_2O_7$ with $Na_4P_2O_7·10H_2O$ addition. *Biomaterials* 1995;**16**(10):793–802.
36. Lin C-C, Liao C-J, Sun J-S, Liu H-C, Lin F-H. Prevascularized bone graft cultured in sintered porous β-$Ca_2P_2O_7$ with 5 wt% $Na_4P_2O_7·10H_2O$ addition ceramic chamber. *Biomaterials* 1996;**17**(11):1133–40.
37. Schneider K, Heimann RB, Berger G. Plasma-sprayed coatings in the system $CaO–TiO_2–ZrO_2–P_2O_5$ for long-term stable endoprostheses. *Mat-wiss u Werkstofftech* 2001;**32**:166–71.
38. Koo J, Bae B-S, Na H-K. Raman spectroscopy of copper phosphate glasses. *J Non-Cryst Solids* 1997;**212**(2–3):173–9.
39. Hudgens JJ, Brow RK, Tallant DR, Martin SW. Raman spectroscopy study of the structure of lithium and sodium ultraphosphate glasses. *J Non-Cryst Solids* 1998;**223**(1–2):21–31.
40. Bamberger CF, Begum GM, Cavin OB. Synthesis and characterization of sodium–titanium phosphates, $Na_4(TiO)(PO_4)_2$, $Na(TiO)PO_4$ and $NaTi_2(PO_4)_3$. *J Solid-State Chem* 1988;**73**(2):317–24.
41. Brow RK, Tallant DR. Structural design of sealing glasses. *J Non-Cryst Solids* 1997;**222**:396–406.
42. Brow RK, Tallant DR, Myers ST, Phifer CC. The short-range structure of zinc polyphosphate glass. *J Non-Cryst Solids* 1995;**191**(1–2):45–55.
43. Tischendorf B, Otaigbe JU, Wiench JW, Pruski M, Sales BC. A study of short and intermediate range order in zinc phosphate glasses. *J Non-Cryst Solids* 2001;**282**(2–3):147–58.
44. Nelson C, Tallant DR. Raman Studies of sodium phosphates with low silica contents. *Phys Chem Glasses* 1985;**26**:119–22.
45. Koudelka L, Mosner P. Study of the structure and properties of Pb–Zn borophosphate glasses. *J Non-Cryst Solids* 2001;**293–295**:635–41.
46. Sakka S, Miyaji F, Fukumi K. Structure of binary $K_2O–TiO_2$ and $Cs_2O–TiO_2$ glasses. *J Non-Cryst Solids* 1989;**112**(1–3):64–8.
47. Fayon F, Massiot D, Suzuya K, Price DL. ^{31}P NMR study of magnesium phosphate glasses. *J Non-Cryst Solids* 2001;**283**(1–3):88–94.